



DIFFERENT EXPOSURE PREDICTION METHODS FOR A WIDE RANGE OF IMPULSIVE NOISES: DO THEY CORRELATE?

Frits van der Eerden * Elisabeth van Pruissen Erik Salomons
TNO - Defense, Safety & Security, The Hague, The Netherlands

ABSTRACT

The auditory risk of temporary or permanent hearing loss is especially high for impulsive noise, such as shooting noise. During military training many different weapons are used, each showing different peak levels and concentration of acoustic energy at different parts of the spectrum. For a safe working environment, the maximum permissible exposure needs to be predicted, taking into account the use of hearing protection. Different prediction methods are available, such as peak and time duration methods, energy methods (ASEL), and model-based methods (such as the electro-acoustic AHAH model). The methods yield different exposure variables, such as ASEL or Auditory Risk Units (ARU's from the AHAH model). Following Murphy *et al* (NIOSH) [1], the correlation between these exposure variables is investigated in this paper, for a wide range of fire arms. Both stylized and more realistic data is processed, gradually increasing in strength. For small fire arms Murphy *et al* have shown that a strong correlation exists, but is this also the case for larger fire arms? An objective of this research is to obtain insight into the performance of exposure prediction methods that are simpler than the model-based methods, without loss of accuracy for predicting hearing loss.

Keywords: *Impulsive noise, Auditory risk, Sound exposure*

1. INTRODUCTION

In this paper a range of impulsive waveforms is introduced, representative for the muzzle blast of light and heavy

*Corresponding author: frits.vandereerden@tno.nl

Copyright: ©2023 First author *et al*. This is an open-access article distributed under the terms of the Creative Commons Attribution 3.0 Unported License, which permits unrestricted use, distribution, and reproduction in any medium, provided the original author and source are credited.

weapons. The waveforms are scaled for different distances and charge sizes and the exposure is calculated with three different methods:

- A-weighted sound exposure level: ASEL
- Auditory risk units using the AHAH model: A_H (ARU)
- The Pfander criterium: N_p (permissible daily impulses)

The AHAH model [2] is used by the MoD in The Netherlands and the Pfander criterium [3] is used by the MoD in Germany. In this paper the unwarned setting of the AHAH model is used.

Pfander uses two parameters of the waveform: the peak and the C-duration of the signal. The use of peak levels, time-duration and/or (total) equivalent sound levels may not be sufficient to assess auditory risk for the large range of weapon noise, from light arms to large caliber weapons. For that reason the physics based AHAH model has been developed. The Auditory Hazard Assessment Algorithm for the Human takes into account the signal transmission from the free field to the cochlear structure. It then calculates the time history of the displacement of the basilar membrane and derives a Damagage Risk Criterion (DRC), expressed in Auditory Risk Units (ARU). The auditory hazard is determined at 23 locations (frequencies) on the basilar membrane and is the squared (upward) displacement, summed over time. For daily use a maximum of 200 ARU's has been empirically derived, so that no compound threshold shifts are expected (TTS and PTS) [2].

In section 2, Friedlander waveforms are used to compare the three exposure prediction methods for assessing auditory risk. Next, in section 3, noise was added to the waveforms to represent measurements more realistically. Section 4 describes results with the same waveforms, but now with a hearing protection device (HPD) applied, as worn in practice.

One would expect that a signal with more energy represents a higher risk. However, the AHAH results show a non-monotonic behaviour. This effect is studied in

more detail in section 5. Finally, conclusions and discussions are given in section 6.

2. STYLIZED WAVEFORMS

The used waveforms for light and heavy weapons are shown in Figure 1. The reference (black line) for light weapons is based on a measured waveform at $r_0 = 10$ m distance from a 7.62 mm rifle. For the heavy weapons it is indicative for a 155 mm muzzle blast or 2 kg TNT eq. explosive.

The energy E_0 , peak pressure P_{pos} and positive phase duration T_{pos} are:

light $P_{pos} = 1.2$ kPa, $T_{pos} = 1.0$ ms, $E_0 = 30$ kJ ($r_0=10$ m)

heavy $P_{pos} = 18$ kPa, $T_{pos} = 4.8$ ms. $E_0 = 18$ MJ ($r_0=10$ m)

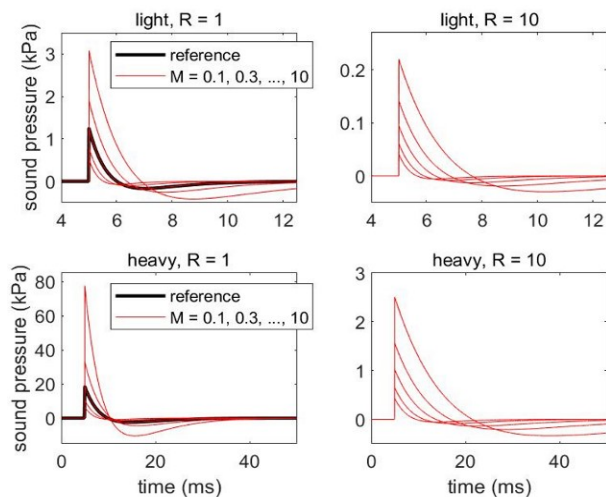


Figure 1. Waveforms for light (top) and heavy (bottom) weapons, using different explosion energies (M) and distance (R).

For the calculation of the waveforms, a point-source explosion model has been used based on numerical results of Brode (1955) and nonlinear propagation theory of Pierce (1991). The model yields the peak pressure and positive phase duration of the Friedlander waveform $p(t) = P_{pos} (1 - t/T_{pos}) \exp(-t/T_{pos})$. The input parameters are the explosion energy and the distance from the point source.

The energy of these reference waveforms are scaled to 3 different distances: $r = R r_0$, with scaling factor $R = 1, 3$ and 10 . And also for 5 different charge energies (or mass): $E = M E_0$, with scaling factor $M = 0.1, 0.3, 1, 3, 10$.

This results in the $2 \times 15 = 30$ waveforms (20 are shown in Figure 1). The sampling frequency is 200 kHz. The corresponding 1/3-octave band spectra for the sound exposure levels (SEL) are shown in Figure 2. For heavy weapons the main frequency is between 16 and 63 Hz, for light weapons it is between 125 and 500 Hz.

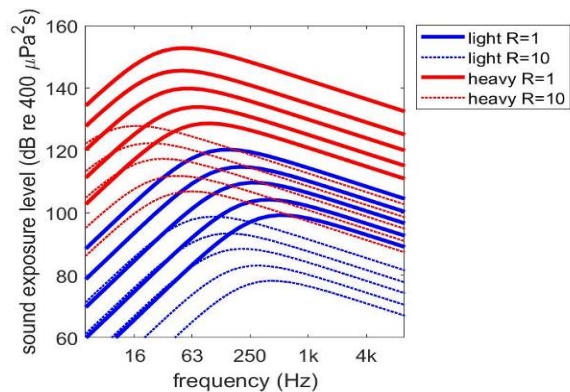


Figure 2. SEL spectra in 1/3-octave bands for 20 different Friedlander waveforms (at 10 and 100 m distance)

The broadband SEL values, unweighted and A-weighted, are depicted in Figure 3. The SEL scales approximately with $10 \log_{10}(M)$. The ASEL values deviate from this linear behaviour because of a decreasing main frequency for an increasing charge energy.

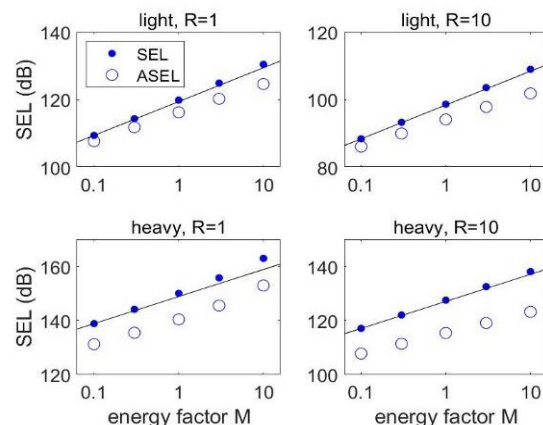


Figure 3. Broadband SEL and ASEL as a function of energy factor M . The black line represents $10 \log_{10} M$.

The 30 ASEL and AHAH results are compared in Figure 4. Values for a fixed distance are connected by

lines, separately for the light and heavy weapons.

For the heavy weapons an increased ASEL results in a linear increase of AHAAH-DRC (using a logarithmic scale). For the light weapons, at 10 and 30 meters distance, a non-monotonic behaviour can be seen. Also, the light weapons show (much) higher ARUs than heavy weapons with similar ASEL values.

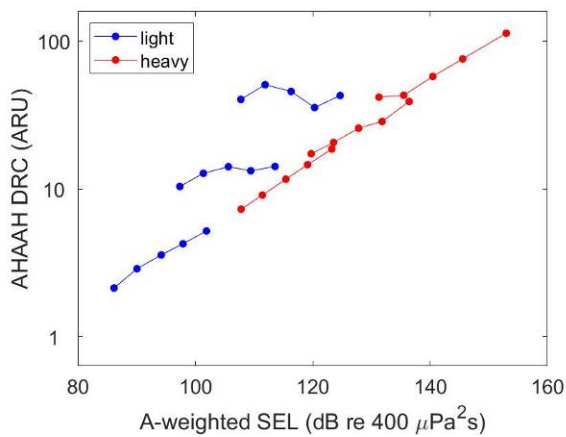


Figure 4. Comparison of ASEL and ARU for 30 waveforms, using a logarithmic axis for the ARU.

The comparison between ASEL and Pfander is shown in Figure 5, with again a logarithmic scale for the vertical axis (using $-10\log_{10} N_p$). For these levels, an approximately linear behaviour with ASEL can be seen.

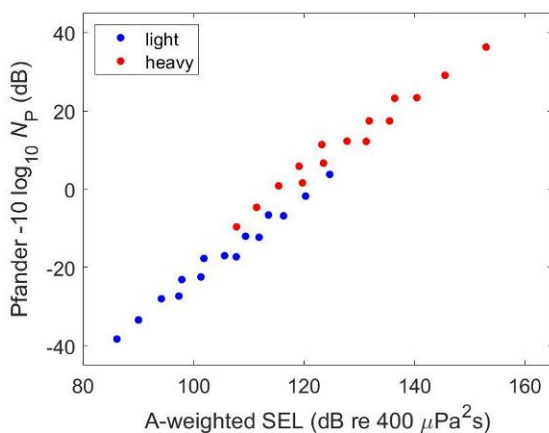


Figure 5. Values of Pfander level $-10\log_{10} N_p$ as a function of ASEL. ($N_p=1$ gives 0 dB, $N_p=100$ gives -20 dB)

3. WAVEFORMS WITH NOISE

Measured waveforms of muzzle blasts and detonations are not so smooth as the Friedlander waveforms and they show a noisy ‘tail’. For a duration of 100 ms, pink noise has been added to the 30 waveforms. The added noise has an rms-amplitude of 2% of the amplitude at the start of the signal and the amplitude decreases linearly to zero at the end. An impression of the first part of the waveforms is given in Figure 6 (compare to Figure 1).

The added noise yields an increase of less than 0.3 dB for the ASEL values and 0.4 dB for the SEL values.

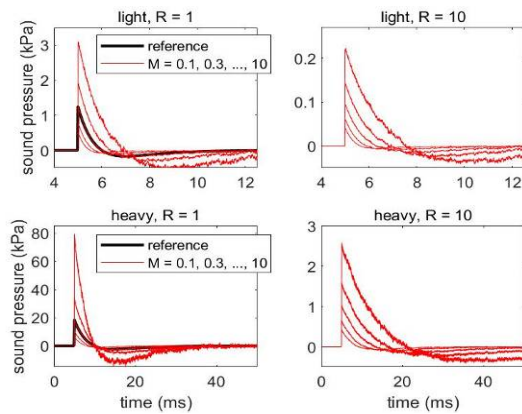


Figure 6. Waveforms of Figure 1 added with pink noise.

The ARU and ASEL results for the waveforms with and without noise are shown in Figure 7, using a logarithmic scale for the ARU.

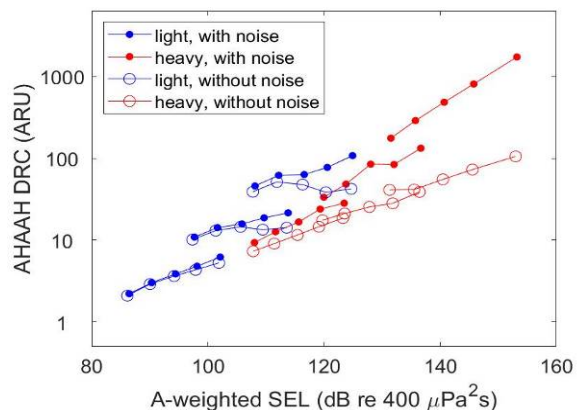


Figure 7. AHAAH-DRC as a function of ASEL for the 30 waveforms without and with added pink noise.

The noisy tail causes the ARU values to increase substantially, especially for the heavy weapons with a factor of more than 10. As a result the correlation between ASEL and ARU shows a more steep slope, when noise is added. Also, the non-monotonic behaviour for the light weapons is not present anymore. In section 5 these results are discussed further.

4. HEARING PROTECTION

In practice hearing protection is used. A standard plug is used here to demonstrate the effect on the ASEL and ARU results. Figure 8 shows the effect of the plug on the spectrum for a light weapon. At low frequencies the attenuation is small and it increases for higher frequencies. In this case ASEL is reduced from 117 to 102 dB.

The HPD module of the AHAAH model calculates the attenuated waveform in the ear canal (filtered in the time domain) and then determines the ARU's at 23 locations of the basilar membrane. The noisy Friedlanders were used for the analysis.

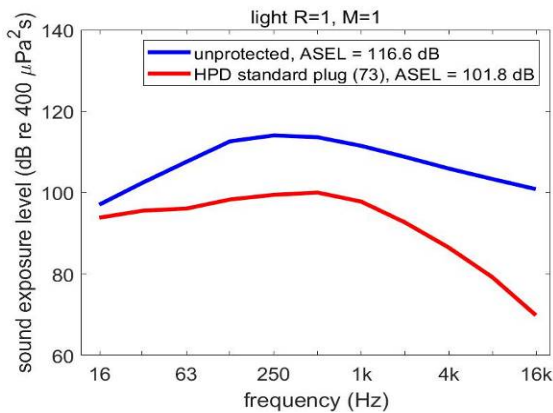


Figure 8. Octave band spectrum for the light weapon ($R=1$, $M=1$) without and with a plug as hearing protection.

The comparison between ASEL and AHAAH-DRC is shown in Figure 9, depicted with the open markers. The results without hearing protection are given with solid markers. The reduction for ASEL is about 13 dB and for the ARU it is about a factor of 100.

Also, for the light weapons the non-monotonic behaviour re-appears (as observed for the Friedlanders without noise in Figure 4).

In the HPD module parameters and values for the electric-acoustic analogue are given to represent the measured attenuation in dB for the plug. The electric parameters are fitted for low, mid and high frequency parts, such that the response matches the measured attenuation values of the HPD. It has been found that different combinations of the electric parameters can be used to represent the same attenuation, which results in different ARUs, up to a factor of 2.

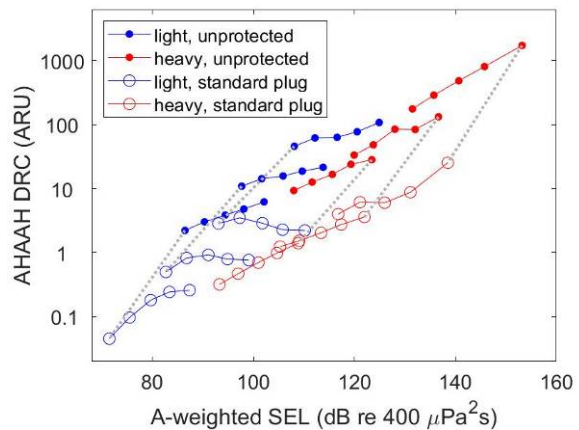


Figure 9. ASEL and ARU results for 30 Friedlanders with a noisy tail, without protection (solid markers) and with a standard hearing protection (plug, open markers).

5. NON-MONOTONIC BEHAVIOUR

To investigate the non-monotonic behaviour of the AHAAH model, the peak pressure and duration of the reference Friedlanders for the light and heavy weapons were changed separately, with scaling factor P for the peak pressure and Q for the positive phase duration:

$$P = 0.1, 0.2, 0.5, 1, 2, 5, 10. \text{ (7 values)}$$

$$Q = 0.1, 0.2, 0.5, 1, 2, 5, 10. \text{ (7 values)}$$

The reference waveforms are repeated here, for the light weapon:

$$P_{\text{pos}} = 1.2 \text{ kPa}, T_{\text{pos}} = 1.0 \text{ ms}, E = 30 \text{ kJ},$$

for the heavy weapon:

$$P_{\text{pos}} = 18 \text{ kPa}, T_{\text{pos}} = 4.8 \text{ ms}, E = 18 \text{ MJ}.$$

The waveforms for the light weapon are shown in Figure 10.

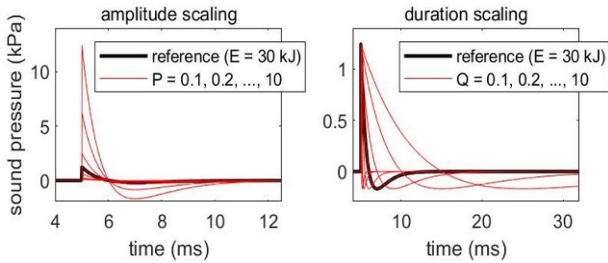


Figure 10. Scaled waveforms for a light weapon, using different peak factors P (left) and time duration factors Q (right).

5.1 Light weapons

The effects of the amplitude and time duration scaling on the SEL and ASEL values are depicted in Figure 11, for light weapons.

The SEL values scale with $20\log_{10} P$ and $10\log_{10} Q$, as expected considering the energy. The ASEL values show a different behaviour for the time duration scaling. For values of $Q > 1$ the increase stops, as a consequence of the spectra shift to lower frequencies (main frequency for $Q=1$ at about 333 Hz, going down to about 166, 67 and 33 Hz for increasing Q).

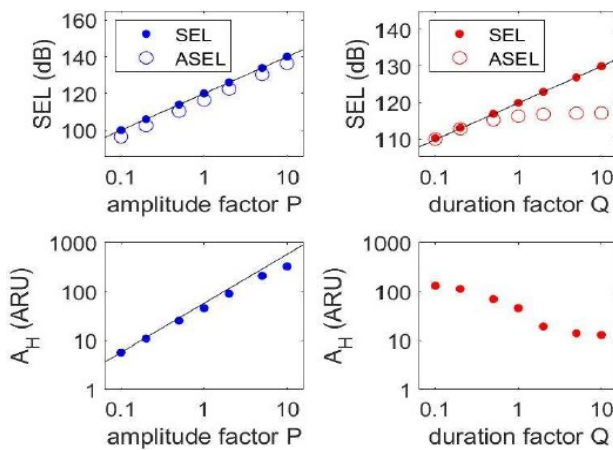


Figure 11. SEL, ASEL and ARU results for light weapons using amplitude and time duration scaling separately.

The lower graphs in Figure 11 show that the ARUs scale linearly with increasing peak pressure. With increasing time durations, the ARUs first decrease by about a factor of 10 and then plateau. This latter effect is comparable to the ASEL results.

In Figure 12 the same scaled waveforms are used to plot ASEL versus AHAAH, using a logarithmic scale for AHAAH. For the different amplitudes there is a linear relation (blue line). However, for the positive phase durations (red line) the behaviour is different. Three values of the duration are indicated in the figure; the dominant frequency decreases by a factor of 100 (about 3000 down to 30 Hz).

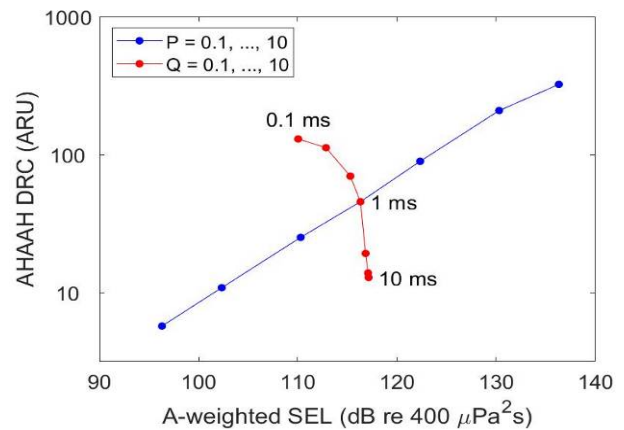


Figure 12. Comparison of ASEL and ARU for amplitude scaled (blue) and time duration scaled (red) waveforms for light weapons.

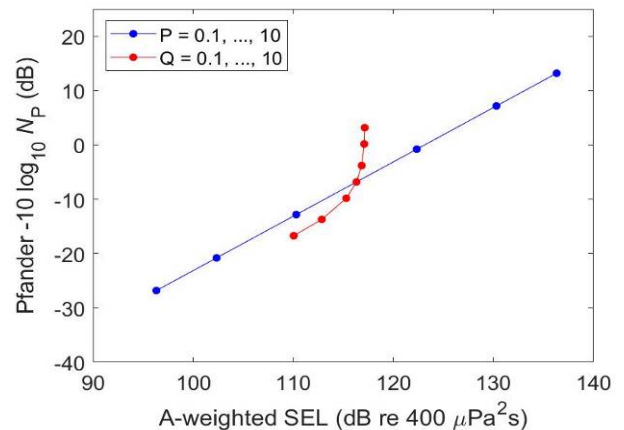


Figure 13. Comparison of ASEL and Pfander for amplitude scaled (blue) and time duration scaled (red) waveforms for light weapons. (N_p ranges from about 50 to 0.5 shots)

As the energy increases for the waveform, the ARUs increase using amplitude scaling, but decrease even stronger for the time duration. It is interesting to look

back at Figures 4 and 9; the non-monotonic behaviour for light weapons originates from the dominating effect of the time duration as the energy increases.

The comparison between ASEL and Pfander (on a logarithmic scale) is given in Figure 13, with a linear relation for the peak scaling and a non-linear one for the time duration. Note that Pfander does not account for A-weighting.

5.2 Heavy weapons

The waveform for the heavy weapon ($E_0 = 18$ MJ) is scaled with amplitude and time duration, similar to the light weapons. Figure 14 shows the SEL spectra for the 7 amplitudes and 7 time durations. The main frequency for $P=1$ and $Q=1$ is about 63 Hz.

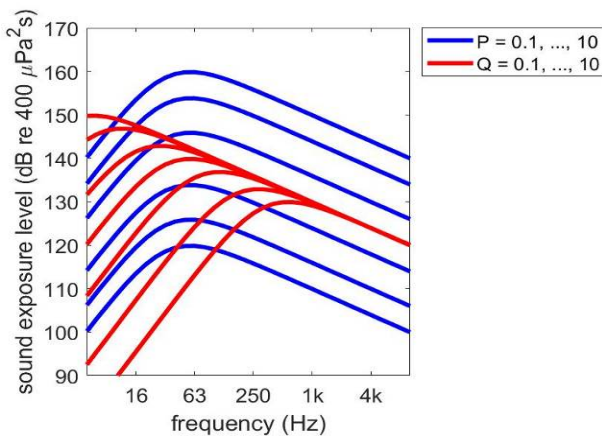


Figure 14. SEL spectra of amplitude scaled (P) and time duration scaled (Q) waveforms for heavy weapons.

The SEL, ASEL and ARU values are given in Figure 15, with a similar behaviour for SEL and ASEL as for the light weapons. Again ASEL remains constant at longer durations as the frequency content above 1000 Hz remains the same (see Figure 14).

For the ARU the increase is not proportional to the amplitude factor P (given by the dashed line), but proportional to the square root of P (solid line). At this stage it is not so clear why this behaviour is different compared to light weapons, it may be the nonlinear behaviour of the annular stapedial ligament.

Figure 16 shows that the behaviour for the time duration is comparable to light weapons, the ARU decrease by a factor of 10 over the range of values for Q , with a steep decrease.

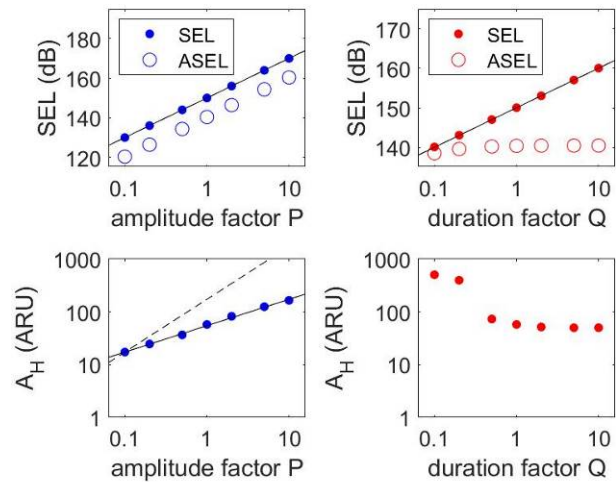


Figure 15. SEL, ASEL and ARU results for heavy weapons using amplitude and time duration scaling separately.

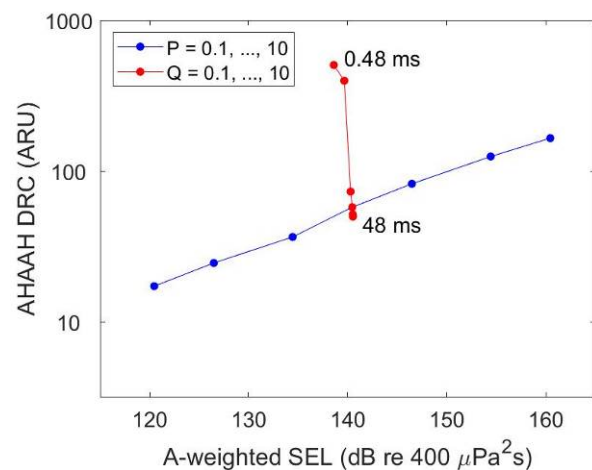


Figure 16. Comparison of ASEL and ARU for amplitude (blue) and time duration scaled (red) waveforms for heavy weapons.

The comparison between ASEL and Pfander in Figure 17 shows a similar behaviour as for light weapons (Figure 13), although the decrease of the number of shots (N_p) is stronger than for light weapons.

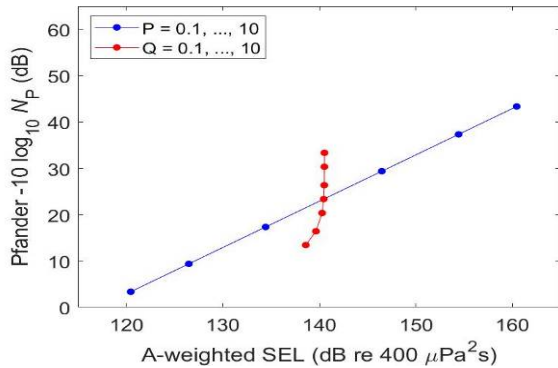
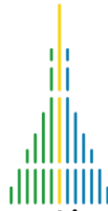


Figure 17. Comparison of ASEL and Pfander for amplitude scaled (blue) and time duration scaled (red) waveforms for heavy weapons. (N_p ranges from about 0.1 to 0.001 shots)

5.3 Weber model waveforms

The non-monotonic behaviour of the AHAH model has been shown by others for different waveforms calculated by the Weber model [3]. They used 19 values of the Weber radius: $R_0 = 0.1, 0.15, \dots, 1.0$ m, representing light weapons increasing in strength. The waveforms have a positive time duration up to 2 ms and a peak amplitude between 164 and 185 dB.

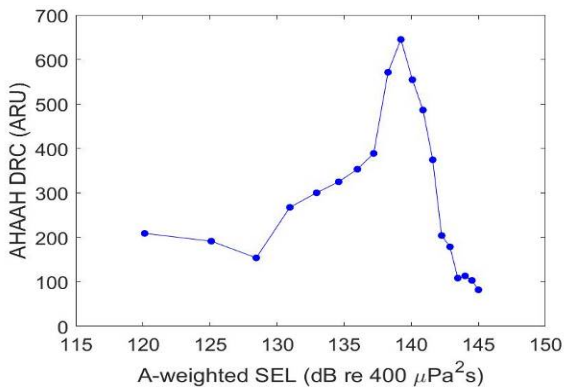


Figure 18. Non-monotonic behaviour for ARU as a function of ASEL and the Weber radius $R_0 = 0.1, 0.15, \dots, 1.0$ m, from left to right. (see also text)

In the original paper [3] Pfander was used on the horizontal axis ($\log_{10}(N_p)$) and ARU on the vertical axis (with a linear scale). This figure could be reproduced. Figure 18 uses ASEL on the horizontal axis, showing almost the exact form as the one with $\log_{10}(N_p)$ on this axis. Note that no noise is added to

the waveforms. The non-monotonic behaviour is similar to the light weapon with the highest ASEL levels depicted in Figure 4.

6. CONCLUSIONS AND DISCUSSION

An objective of this research is to obtain insight into correlation between exposure prediction methods for impulses from light to heavy weapons. Three methods are used: ASEL (energy based), Pfander (using peak and time duration) and AHAH (based on a model of the ear).

There is a good (linear) correlation between ASEL and Pfander for the range of impulses used. Differences are found when only the main frequency of the spectrum is changed (lower than 1000 Hz) due to the effect of A-weighting that is not present in the Pfander method.

There is no simple correlation between AHAH and ASEL:

- it is different for light and heavy weapons,
- a non-monotonic behaviour is seen,
- AHAH is very sensitive to noise

On one hand, the behaviour of AHAH may reflect that it should be restricted to the very loud impulses (SPLs of 150 dB and higher), although the authors claim that the model may be applied to free field exposures above 115 to 120 dB.

When applying hearing protection, the sound levels may be lower than 115 dB. For a standard plug, it was shown that ASEL was reduced by about 15 dB and ARU by a factor of 100.

On the other hand, the AHAH model accounts for different mechanisms that are present in the ear, such as the non-linear behaviour of the annular stapedial ligament, and the response in the time-domain at 23 positions of the basilar membrane. It can be used for a wide range of impulses.

The minor oscillations of the sound pressure, introduced as a noisy tail (0.3 dB increase), apparently caused oscillations of the basilar membrane that result in a large increase of the hearing damage risk (ARU more than 10 times higher).

The AHAH model accounts only for upward motions of the membrane. It would be interesting to see if the modified AHAH model, proposed by

Zagadou et al [4], would provide similar results, as it is based on the cochlear energy. This is work in progress.

Zagadou et al demonstrated that the non-monotonic behaviour is no longer present when using the cochlear energy instead of the upward vibrations of the membrane. But animal studies by Price (1983) and Dancer (1985) showed that the damage risk for large caliber weapons can be lower compared to small caliber weapons; the effect of long-duration impulses could be smaller than those from shorter duration at the same peak level, although the energy contained in an impulse increases with duration [5].

A copy of a figure by Dancer et al is given in Figure 19. It shows the hearing loss (TTS) in guinea pigs as a function of frequency for Friedlander waves with 4 different positive phase durations: 0.05, 0.25, 0.39 and 1.0 ms (denoted as M, B, O, N) and constant peak pressure.

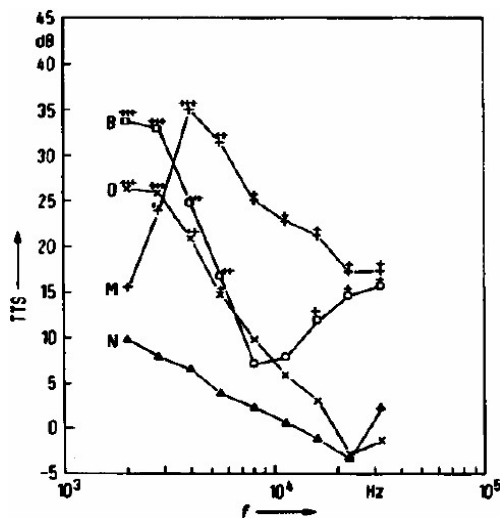


Figure 19. Copied from Dancer et al (1985). Measured hearing loss (TTS) in guinea pigs as a function of frequency for Friedlander waves with 4 different positive phase durations: 0.05, 0.25, 0.39 and 1.0 ms (denoted as M, B, O, N).

It is demonstrated that the TTS for an increased duration can be less although the acoustic energy at is not decreased. This is argued as an essential aspect of the AHAH model.

Longer duration waveforms results in a spectral shift that has a different effect on ASEL, Pfander and

AHAH. The ARUs show a strong reduced risk, the A-weighted hearing shows a plateau, and Pfander shows an increased risk. It has been shown that ARU decreases as a function of ASEL if the waveform duration is increased from 0.1 to 10 ms (light weapons) or from 0.45 ms to 48 ms (heavy weapons).

The reason for the different behaviour of the AHAH model is hidden in the details of the electrical analogue approach. It would be valuable to have a better understanding or validation of this behaviour.

As a final remark, the focus in this paper is not on the maximum allowable shots, but on the correlation between the three exposure prediction methods when using a single shot. In addition, the challenge lies in getting a good exposure response function (impulse versus TTS), especially at lower exposures and/or TTS. For instance, one can easily set a daily limit for one exposure method (e.g. ASEL) if it correlates with an alternative exposure method (e.g. AHAH).

7. ACKNOWLEDGMENTS

This work is done in the MoD-NL research program V2204 “Soldier Protection from military Health Threats” and in the TA 38 between MoD-NL and Mod-GE on “Hearing damage risk of shooting noise to personnel & underlying damage risk criteria”. The cooperation with MoD-NL CEAG, MoD-GE WTD91, ISL and Cervus Consult is acknowledged.

8. REFERENCES

- [1] W. J. Murphy, G. A. Flamme, E. B. Brokaw, R. K. Gupta, “Acoustic standards for high-level impulse noise”, JASA 148, 2020. (presentation via research-gate.net)
- [2] G. R. Price and J. T. Kalb, “The Philosophy, Theoretical Bases, and Implementation of the AHAH Model for Evaluation of Hazard from Exposure to Intense Sounds”, United States Army Research Laboratory, ARL-TR-8333, Apr. 2018.
- [3] C. Hudasch, P. Bechtel, K. Hirsch, C. Kleinhenrich, T. Langenburcher, “Das Pfander-Kriterium im Vergleich zum Gehörgefährdungsindex des AHAH-Modells”, DAGA 2020
- [4] B. Zagadou, P. Chan, K. Ho, D. Shelley, “Impulse noise injury prediction based on the cochlear energy”, Elsevier, Hearing Research, 2016.
- [5] R. Drullman (editor), “Reconsideration of the effects of impulse noise”, TM-02-1012, Final Report of NATO Research Study Group RSG.29 (Panel 8 – AC/243), Dec. 2002